

**SINTAP/TWI/012  
MARCH 1999**

**EFFECT OF CRACK TIP  
CONSTRAINT ON FRACTURE  
TOUGHNESS OF A533B STEEL  
AND VALIDATION OF THE  
SINTAP CONSTRAINT  
PROCEDURE**

**For: Task 2**

**EFFECT OF CRACK TIP CONSTRAINT ON FRACTURE  
TOUGHNESS OF A533B STEEL AND VALIDATION OF THE  
SINTAP CONSTRAINT PROCEDURE**

**TWI REPORT NO: SINTAP/TWI/012  
MARCH 1999**

Prepared for: Sintap Task 2

Contact: R Ainsworth  
Nuclear Electric Ltd  
Barnett Way  
Barnwood  
Gloucester  
GL4 3RS

Prepared by: I Hadley and S A Karger

## CONTENTS

<b>EXECUTIVE SUMMARY</b>	<b>i</b>
<b>Background</b>	<b>i</b>
<b>1. INTRODUCTION</b>	<b>1</b>
<b>2. OBJECTIVES</b>	<b>1</b>
<b>3. METHOD</b>	<b>2</b>
<b>4. RESULTS AND DISCUSSION</b>	<b>3</b>
<b>4.1. RAW DATA</b>	<b>3</b>
<b>4.2. COMPARISON WITH OTHER DATA</b>	<b>4</b>
<b>4.3. CALCULATION OF CONSTRAINT PARAMETERS FOR SENB SPECIMENS</b>	<b>4</b>
<b>4.4. ANALYSIS OF WIDE PLATE TEST DATA</b>	<b>5</b>
<b>4.4.1. Analysis using a Conventional FAD</b>	<b>6</b>
<b>4.4.2. Modification of <math>K_r</math></b>	<b>6</b>
<b>4.4.3. Modification of the FAD</b>	<b>8</b>
<b>4.5. OVERALL DISCUSSION</b>	<b>9</b>
<b>5. CONCLUDING REMARKS</b>	<b>10</b>
<b>6. REFERENCES</b>	<b>11</b>
<b>TABLES</b>	
<b>APPENDICES</b>	

# EFFECT OF CRACK TIP CONSTRAINT ON FRACTURE TOUGHNESS OF A533B STEEL AND VALIDATION OF THE SINTAP CONSTRAINT PROCEDURE

## EXECUTIVE SUMMARY

### Background

Appendix 3 of the SINTAP procedure and Appendix 14 of the CEGB's R6 procedure describe methods of including in-plane constraint in the analysis of structures containing flaws. As part of an effort to validate these procedures, TWI has carried out a series of shallow-crack fracture mechanics tests on a grade A533B steel. Testing was carried out at  $-100^{\circ}\text{C}$  so as to be able to apply the data to a series of biaxial and uniaxial wide plate test results. The results from both the small-scale single edge-notched bend (SENB) specimens and the large-scale centre-cracked tension (CCT) wide plate tests were indexed in terms of the fracture parameters  $J$  and CTOD and the constraint parameter  $T/\sigma_Y$ .

### Conclusions

A strong effect of in-plane constraint on fracture toughness was demonstrated; shallow-crack specimens failed at critical values of  $J$  up to four times higher than the value associated with deeply-notched specimens. Shallow-crack specimens also showed larger amounts of ductile tearing prior to fracture. When results were indexed in terms of the constraint parameter  $T/\sigma_Y$ , results of both the SENB and CCT tests were shown to lie on a single curve, as implied by Procedure II of R6, Appendix 14.

Procedure I (application of a constraint-based FAD) was also applied. In this case, it was more difficult to apply than Procedure II, because of the very steep rise in fracture toughness associated with negative  $T/\sigma_Y$ . Nevertheless, the constraint-based procedure correctly predicted the failure of the CCT specimens, provided that lower-bound values of CTOD fracture toughness were used.

# EFFECT OF CRACK TIP CONSTRAINT ON FRACTURE TOUGHNESS OF A533B STEEL AND VALIDATION OF THE SINTAP CONSTRAINT PROCEDURE

## 1. INTRODUCTION

Defect assessment procedures such as the CEGB's R6 procedure<sup>1</sup> and BSI's procedures PD6493<sup>2</sup> and BS7910<sup>3</sup> rely on accurate measurement of fracture toughness ( $K_{Ic}$ , J or CTOD) using standard deeply-notched bend specimens. These standard specimens tend to give safe (conservative) predictions of failure conditions, since fracture toughness is measured under conditions of high crack tip constraint. Given that engineering structures containing cracks are likely to be loaded predominantly in tension and to contain only shallow cracks, there is now considerable interest in deriving methods for incorporating crack-tip constraint into defect assessment procedures. For example, Appendix 14 of the CEGB R6 procedure and Appendix 3 of the draft SINTAP procedure<sup>4</sup> outline a method for incorporating constraint effects into the FAD (Failure Analysis Diagram). In essence, the requirement is to measure fracture toughness under a variety of different constraint conditions, and so to formulate a relationship between fracture toughness and a constraint parameter such as the elastic T-stress.

In 1996, TWI<sup>5</sup> reviewed the large-scale test programmes which it had carried out for the NII and power utilities over the previous 12 years, with a view to interpreting the results in terms of constraint models such as R6 Appendix 14. It was shown that the series of biaxial wide plate (WP) tests on A533B steel were of particular interest in this respect, for the following reasons:

1. The tests covered a range of crack types and loading conditions. As well as conventional small-scale tests, surface-cracked and through-cracked wide plate specimens had been tested under both biaxial and uniaxial loads.
2. Extensive analysis of the dataset using a conventional FAD and standard small-scale fracture toughness tests had already been carried out.
3. A strong effect of biaxiality on fracture of through-cracked plates in the lower transition was predicted by numerical modelling and confirmed by experiment<sup>6-11</sup>.
4. The tests were carried out on parent plate, so the effects which complicate interpretation of welded structures (e.g. secondary stresses, secondary bending, materials mismatch and microstructural changes) could be ignored in the first instance.

It was considered that the results of this test programme would provide an excellent opportunity to validate the constraint-based FAD approach. However, all small-scale testing hitherto carried out on the steel used conventional deeply-notched specimens. A limited programme of small-scale testing under low-constraint conditions was therefore carried out to fill this gap.

## 2. OBJECTIVES

The objectives of the project were:

- to determine the dependence of the fracture toughness of A533B steel at  $-100^{\circ}\text{C}$  on in-plane constraint by varying the crack depth of SENB specimens,

## EFFECT OF CRACK TIP CONSTRAINT ON FRACTURE TOUGHNESS OF A533B STEEL AND VALIDATION OF THE SINTAP CONSTRAINT PROCEDURE

- to apply Appendix 3 of the draft SINTAP procedure (similar to Appendix 14 of R6) to interpret the results of a series of wide plate tests

### 3. METHOD

A series of small-scale fracture mechanics tests was carried out on A533B material (see Appendix 1 for details of chemical composition and properties). Conditions for the test were designed to match those of a series of wide plate tests<sup>5</sup> on through-thickness-notched specimens, i.e.

- test material identical to that used in the wide plate tests,
- test temperature  $-100^{\circ}\text{C}$ ,
- specimen orientation L-T,
- specimen thickness 50mm.

In order to produce different constraint conditions, the ratio of crack depth ( $a_o$ ) to specimen width ( $W$ ) was varied between 0.1 and 0.5. Special procedures for testing and analysis of shallow crack specimens were used for all specimens, based on Ref. 12 and 13. In particular, the relationship between applied load and CMOD (Crack Mouth Opening Displacement) was recorded during the test and the area under the load/CMOD curve (designated  $A_c$ ) was calculated. The value of  $J$  at fracture,  $J_q$ , was then calculated<sup>13</sup> from:

$$J_q = \frac{K^2 (1 - \nu^2)}{E} + \eta_c \frac{A_c}{Bb} \quad [1]$$

where:

$$\eta_c = 3.785 - 3.101 \frac{a_o}{W} + 2.018 \left( \frac{a_o}{W} \right)^2$$

$b$  = specimen ligament,  $(W - a_o)$ , mm

$B$  = specimen thickness, mm

$K$  is as defined in BS 7448

The shallow-crack value of CTOD,  $CTOD_q$  was calculated from Eq.[2] as follows:

$$CTOD_q = \frac{J_q}{m\sigma_f} \quad [2]$$

where  $\sigma_f$  is the material flow strength at the test temperature, and

$$m = 1.221 + 0.793 \left( \frac{a_o}{W} \right) + 2.751n - 1.418n \left( \frac{a_o}{W} \right) \quad [3]$$

## EFFECT OF CRACK TIP CONSTRAINT ON FRACTURE TOUGHNESS OF A533B STEEL AND VALIDATION OF THE SINTAP CONSTRAINT PROCEDURE

where  $n$  is the work-hardening coefficient of the material, either determined from a measured stress-strain curve or estimated from the ratio ( $R$ ) of ultimate tensile strength to the yield strength as follows:

$$n = 1.724 - \left( \frac{6.098}{R} \right) + \left( \frac{8.326}{R^2} \right) - \left( \frac{3.965}{R^3} \right) \quad [4]$$

Results for deeply-notched specimens ( $a_0/W \approx 0.5$ ) were assessed as above, but were also interpreted using the conventional formulae for  $J$  and CTOD, as given in BS 7448:Part 1:1991 (using the area under the load-displacement curve,  $U_p$ , to calculate the plastic component of  $J$ ).

### 4. RESULTS AND DISCUSSION

#### 4.1. RAW DATA

Results of the fracture mechanics tests are shown in Table 1 and Appendix 1. For deeply-notched specimens, the values of toughness are shown in terms of both the conventional toughness parameters ( $J_{BS}$  and  $CTOD_{BS}$ ) and the parameters calculated from the shallow crack formulae ( $J_q$  and  $CTOD_q$ , see Eq.[1] and [2]). Some results on deeply-notched specimens, available from a previous project<sup>5</sup>, are also included for completeness; note that these tests were carried out on a rectangular-section (50x100mm) specimens rather than the square-section (50x50mm) specimens used in the main part of the current project.

Figure 1 shows the relationship between  $a_0/W$  and the value of  $J$  at fracture ( $J_{BS}$  or  $J_q$ ). Only under conditions of very low constraint ( $a_0/W \approx 0.1-0.2$ ) is there a large rise in critical  $J$ ; values for intermediate crack depths ( $0.2 < a_0/W < 0.5$ ) are fairly insensitive to crack depth. There is an increase in fracture toughness by a factor of between three and four between the deeply-cracked and shallow-cracked specimens, i.e.  $J_{a/W=0.1}/J_{a/W=0.5} \approx 3.4$ . It is also evident from Fig.1 and Table 1 that the majority of shallow-crack specimens (seven of the twelve specimens having  $a_0/W < 0.2$ ) failed after undergoing more than 0.2mm of ductile tearing.

Figure 2 shows the relationship between fracture toughness and the amount of ductile tearing for all categories of specimen, with  $0.1 < a_0/W < 0.5$ . The increasing value of fracture toughness is seen to be strongly dependent on the amount of ductile tearing,  $\Delta a$ , which in turn is dependent on the crack depth  $a_0/W$ . Low constraint thus appears to raise the cleavage toughness to beyond the level at which ductile tearing initiates – consequently, cleavage failure in low-constraint specimens occurs only after some ductile tearing.

An effect of constraint on fracture toughness has therefore been demonstrated by this work, but the effect (an increase in fracture toughness by a factor of around 3.4) is dominated by an increased amount of ductile tearing prior to cleavage failure. If the results shown in Fig.1 are censored to exclude  $J_u$  results (those with more than

## EFFECT OF CRACK TIP CONSTRAINT ON FRACTURE TOUGHNESS OF A533B STEEL AND VALIDATION OF THE SINTAP CONSTRAINT PROCEDURE

0.2mm of ductile tearing on the surface), the effects of constraint on toughness would be considerably lower.

Significant amounts of stable ductile tearing were not expected in these tests, because the test temperature (-100°C) was close to the lower shelf region of the ductile-brittle transition curve for deeply-notched specimens (see Fig.3). It may be that the onset of tearing would not have occurred (even in shallow-notch specimens), had tests been carried out at a lower temperature. However, this possibility was not examined under the current programme, since the test temperature was dictated by the temperature at which wide plate test results were available, i.e. -100°C.

### 4.2. COMPARISON WITH OTHER DATA

The results of these tests may be compared with those reported by Smith and Rolfe as part of the US Heavy-Section Steel Technology (HSST) programme<sup>14</sup>. Smith and Rolfe report fracture toughness of a similar A533B reactor steel, but only under conditions of very high ( $a_0/W=0.5$ ) and very low ( $a_0/W=0.1$ ) constraint conditions. They show the ratio  $J_{a/W=0.1}/J_{a/W=0.5}$  to be around 8.7 for 20mm thick specimens tested at -104°C. However, the nine-fold increase in fracture toughness which they observed was not associated with ductile tearing, but with cleavage fracture only. To date, no metallurgical comparisons have been made between the two steels.

### 4.3. CALCULATION OF CONSTRAINT PARAMETERS FOR SENB SPECIMENS

In order to apply constraint-sensitive defect assessment procedures such as Appendix 14 of the CEGB R6 procedure and Appendix 3 of the draft SINTAP procedure, the results of Fig.1 need to be re-indexed in terms of either the elastic T-stress or Q-stress ( $T/\sigma_Y$  or  $Q/\sigma_Y$ ). The procedure described in Ref.15/16 was used, in which the relative collapse load,  $L_r$ , is first calculated; a T-stress route is followed for  $L_r < 1$ , or a Q-stress route for  $L_r > 1$ .

- The plane strain limit load,  $P_L$ , was first calculated from:

$$P_L = \sigma_L \frac{BW^2}{1.5S} \quad [5]$$

where:

$$\sigma_L = 1.21\sqrt{3}\sigma_Y \left(1 - \frac{a}{W}\right)^2 \quad [6]$$

and  $L_r$ , the ratio of failure load ( $P_f$ ) to limit load ( $P_L$ ) was calculated for each specimen.

## EFFECT OF CRACK TIP CONSTRAINT ON FRACTURE TOUGHNESS OF A533B STEEL AND VALIDATION OF THE SINTAP CONSTRAINT PROCEDURE

- the constraint parameter  $\beta_T$  was calculated. Values of  $\beta_T$  were calculated from the polynomial given in Ref.16:

$$\beta_T = 0.23 - 19.3 \frac{a}{W} + 150.3 \left( \frac{a}{W} \right)^2 - 472.8 \left( \frac{a}{W} \right)^3 + 736.3 \left( \frac{a}{W} \right)^4 - 560.3 \left( \frac{a}{W} \right)^5 + 165.6 \left( \frac{a}{W} \right)^6 \quad [7]$$

- $\beta_Q$  was estimated from the graphical solutions given in Ref.16, assuming  $n=10$  (calculated from Eq.[4] above).

The full results are given in Appendix 1, Table A1. Values of  $L_r$  at failure fell in the range  $0.734 < L_r < 1.058$  and all results were plotted as a function of both  $\beta_T L_r$  and  $\beta_Q L_r$  (see Fig.4 and 5). The trends in results are broadly similar, with higher values of  $J$  associated with negative values of  $\beta_T L_r$  and  $\beta_Q L_r$ . A Q-stress-based analysis distinguishes better than a T-stress-based approach between the three specimens (No. M01-09, -11, and -15) failing at high values of  $J$  and  $L_r > 1$ . Ultimately, since very few of the specimens tested (three out of the 20 BxB specimens) failed with  $L_r > 1$ , subsequent analyses were carried out using the elastic T-stress approach only.

#### 4.4. ANALYSIS OF WIDE PLATE TEST DATA

One of the objectives of the project was to use the shallow-crack tests to predict the results of a series of wide plate tests carried out on the same material<sup>5-11</sup> by TWI, and thus to check the validity of the proposed SINTAP constraint analysis procedure. Previous numerical analysis<sup>18</sup> of centre-cracked tension-loaded plates (CCT specimens) predicted that the apparent toughness of the plates at temperatures corresponding to the lower shelf would depend on the biaxiality ratio  $k$ . [The parameter  $k$  is the ratio of the stress parallel to the crack to the stress perpendicular to the crack; consequently  $k=0$  for a uniaxially loaded plate,  $k=1$  for equibiaxial loading (e.g. the stress state in a spherical pressure vessel)]. Two additional loadcases were also considered, namely  $k=0.5$  and  $k=2.0$ , corresponding to the stress states experienced by the longitudinal and circumferential seams of a cylindrical pressure vessel. The predictions of the numerical analyses are shown in Fig.6; a strong effect of biaxiality was predicted, which was subsequently confirmed by testing. Table 2 shows the experimental results, in terms of failure stress and CTOD at failure (note that specimen M01-27 was effectively tested twice, once under  $k=2$  conditions where failure did not occur at an applied CTOD of 0.05mm, and then retested under  $k=0.5$ ). It can be seen that the CTOD at failure for the uniaxially loaded plate ( $k=0$ ) is some three to four times higher than that measured in the equibiaxially loaded ( $k=1$ ) plate, and 2.3 times higher than the average CTOD measured on deeply-notched SENB specimens. The magnitude of the elevation in fracture toughness for the uniaxial wide plate specimen relative to the deeply-notched SENB specimen is, in fact, very close to that reported in Section 4.1 for the ratio  $J_{a/W=0.1}/J_{a/W=0.5}$ .

The results of two tests, the uniaxial and equibiaxial, are re-interpreted here, firstly using a conventional FAD, then the two constraint-based procedures proposed in R6 Appendix 14/SINTAP Appendix 3.

#### **4.4.1. Analysis using a Conventional FAD**

Figure 7 shows the outcome of an analysis of the uniaxial wide plate test ( $k=0$ ). This was analysed in the conventional manner, using a standard FAD and deeply-notched fracture mechanics specimens. Lower-bound fracture toughness values of  $J=107.9\text{kJ/m}^2$  ( $K_J=157.8\text{MPa}\sqrt{\text{m}}$ ) and  $\text{CTOD} = 0.11\text{mm}$  were used in deriving this diagram, being the lowest of the three results from deeply notched 50x50mm SENB specimens, analysed in accordance with BS 7448. [Lumping the three deeply notched 50x50mm specimens and the three 50x100mm specimens together and taking the second lowest result would have given virtually identical results.]

The analysis was carried out in accordance with the draft procedure BS7910<sup>3</sup> to Level 2, using a material-specific failure-assessment line derived from low-temperature tensile tests on the material in question. The procedure used is therefore similar to PD6493<sup>2</sup> Level 2, except that the x-axis is based on  $L_r$  instead of  $S_r$ , and the failure-assessment line is specific to the material under test. The analysis was simplified somewhat by ignoring as a first approximation the effects of secondary stresses such as thermal and bending stresses.

Results (see Appendix 2 for full analysis details) show that failure is safely predicted from the conventional FAD-based approach, with a somewhat higher margin of safety for CTOD-based results than for  $K_J$ -based; this is in line with previous experience<sup>18</sup>.

An additional datapoint in Fig.7 shows that a conventional K-based analysis based on the mean fracture toughness under high constraint conditions lies only marginally outside the FAD. This underlines the importance of using lower-bound fracture toughness in any analysis.

Analysis of the equibiaxial wide plate test will be considered in Section 4.4.2, since it is immediately clear from Table 2 that the CTOD at failure of the biaxially loaded plate was very similar to that of the SENB specimens.

#### **4.4.2. Modification of $K_r$**

Procedure II of R6 Appendix 14 requires calculation of the constraint parameter  $\beta$  ( $\beta_T$  or  $\beta_Q$ ) for the wide plate specimens, using a procedure similar to that described in Section 4.3 for the SENB specimens.  $\beta_T L_r$  is then used as a measurement of structural constraint, and the material toughness  $K_{\text{mat}}$  is predicted to be a function of  $\beta_T L_r$  for all types of specimen. In essence, Procedure II re-defines the toughness of the 'structure' (in this case, a wide plate specimen) as equivalent to that of a small-scale specimen with matching crack-tip constraint. A standard FAD is then used to predict the behaviour of the structure, using the 'constraint-matching' value of fracture toughness in place of the lower bound high-constraint toughness.

The parameters  $L_r$ ,  $\beta_T$  were calculated from the solutions given in Ref.16 for both the centre-cracked, uniaxially loaded plate and a biaxially loaded plate as follows:

**EFFECT OF CRACK TIP CONSTRAINT ON FRACTURE TOUGHNESS OF A533B STEEL AND VALIDATION OF THE SINTAP CONSTRAINT PROCEDURE**

- For the centre-cracked (uniaxially loaded) plate:

$$\sigma_L = \frac{2\sigma_Y}{\sqrt{3}} \left(1 - \frac{a}{W}\right) \quad [8]$$

and

$$\beta_T = -1.2253 + 2.2691 \frac{a}{W} - 6.867 \left(\frac{a}{W}\right)^2 + 13.065 \left(\frac{a}{W}\right)^3 - 8.6481 \left(\frac{a}{W}\right)^4 \quad [9]$$

- For the centre-cracked (biaxially loaded) plate ( $a/W < 0.5$  only):

$$\sigma_L = \frac{2\sigma_Y}{\sqrt{3}} \quad [10]$$

and

$$\beta_T = -0.02420 - 0.29309 \frac{a}{W} + 0.91749 \left(\frac{a}{W}\right)^2 - 10.021 \left(\frac{a}{W}\right)^3 - 12.695 \left(\frac{a}{W}\right)^4 \quad [11]$$

For the  $k=0.5$  and  $k=2$  cases, handbook values of  $L_T$  are not available, but the value  $T/\sigma_Y$  was obtained directly from a finite element analysis of the actual wide plate test conditions, as reported in Ref.19. An additional estimate was made by calculating  $T/\sigma_Y$  directly from the dimensionless elastic  $T/\sigma$  functions due to Kfourri (given in Ref.17) and the nominal stress at failure.

Table 3 shows the constraint parameters for each geometry; there is a reasonable match between the 'handbook' and FEA solutions for the cases  $k=0$  and  $k=1$ . The FEA solution is potentially more accurate, being based on the actual geometry of a specific wide plate specimen.

The toughness of all specimens (in terms of CTOD) is plotted in Fig.8 as a function of the constraint parameter  $T/\sigma_Y$  or  $\beta_T L_T$ . All points can be seen to collapse onto a single curve, as postulated by Procedure II of Appendix 14. The points corresponding to the biaxial wide plate tests ( $k=0.5, 1.0$  and  $2.0$ ) lie within the scatter band for the SENB specimens, whereas the uniaxial ( $k=0$ ) wide plate specimen does appear to have slightly higher toughness than do the corresponding SENB specimens at an equivalent level of constraint ( $T/\sigma_Y \approx 0.5, a/W \approx 0.15$ ).

The wide plate results described in Ref.5-11, plus the three Bx2B deeply-notched results shown in Fig.8, are available in terms of CTOD only. However, a value of  $J$  at fracture for the uniaxial wide plate was retrospectively determined for this project

## EFFECT OF CRACK TIP CONSTRAINT ON FRACTURE TOUGHNESS OF A533B STEEL AND VALIDATION OF THE SINTAP CONSTRAINT PROCEDURE

using the method described in Ref.20. Results are shown in Fig.9; the uniaxial wide plate test results are seen to lie on the same curve as the SENB data, once all data are indexed by the constraint parameter.

An approximate lower bound value to the toughness curve at  $T/\sigma_Y \approx -0.5$  (the constraint parameter corresponding to the conditions of the uniaxial wide plate test) is  $CTOD=0.18\text{mm}$ ,  $J=155\text{kJ/m}^2$  ( $K_J=189\text{MPa}\sqrt{\text{m}}$ ). If the behaviour of the uniaxial wide plate test is re-analysed using low-constraint values of fracture toughness (from the shallow-crack SENB specimens), then the analysis points (see Fig.10) can be seen to lie much closer to the failure analysis line than was the case when a standard high-constraint analysis was used (compare Fig.7 and 10). In fact, the point associated with the  $K_J$ -based analysis lies just inside the failure analysis line, indicating a safety factor of approx. one on the analysis. It should be noted that the values of fracture toughness used are lower bound values for a particular constraint condition, in line with the procedures used for standard FAD-based analysis.

The analysis of the uniaxial wide plate test, carried out in accordance with Procedure II of Appendix 14 (modification of  $K_r$ ) has thus shown that application of a constraint-based model can lead to a more accurate prediction of failure conditions than would be possible using the standard high-constraint FAD-based model.

The results of applying the same procedure to the equibiaxial test are shown in Fig.11. The driving force in this case included secondary stresses, derived from a thermal analysis<sup>11</sup>. As seen in Fig.7, the lower bound value of toughness at  $T/\sigma_Y \approx 0.0$  (the constraint parameter appropriate to the equibiaxial test) is approximately  $CTOD=0.11\text{mm}$  or  $J=108\text{kJ/m}^2$  ( $K_J=158\text{MPa}\sqrt{\text{m}}$ ), equal to the conventional lower-bound toughness described in Section 4.4.1. The analysis produces two points – a CTOD-based point far outside the failure analysis line and a  $K_J$ -based point just outside it.

### 4.4.3. Modification of the FAD

The alternative method (termed procedure I in Appendix 16 of R6) for incorporating constraint effects into a fracture analysis procedure is to modify the Failure Analysis Diagram to take account of the constraint, and to consider the toughness of the material constant, as measured by the high-constraint value of fracture toughness,  $K_{\text{mat}}$ .

This procedure requires the fracture toughness to be expressed as a function of the constraint parameter, i.e.  $K_r=f(L_r)(K_{\text{mat}}^c/K_{\text{mat}})$  for  $L_r \leq L_r^{\text{max}}$ . A relationship of the form:

$$K_{\text{mat}}^c = K_{\text{mat}} [1 + \alpha(-\beta_T L_r)^m]$$

was derived as shown in Fig.12. The values  $K_{\text{mat}}=180\text{MPa}\sqrt{\text{m}}$ ,  $\alpha=14.4$ ,  $m=5.52$  were first calculated over the whole dataset, using Matlab software. In view of the scatter in the data, together with the sharp rise in fracture toughness when  $T/\sigma_Y$  is

## EFFECT OF CRACK TIP CONSTRAINT ON FRACTURE TOUGHNESS OF A533B STEEL AND VALIDATION OF THE SINTAP CONSTRAINT PROCEDURE

very negative, application of this method is somewhat more difficult than Procedure II. In particular, the values of  $\alpha$  and  $m$  are likely to be highly sensitive to small changes in the input data. Procedure II appears to be both more intuitive and easier to apply than Procedure I in this case.

A second relationship between  $K_{mat}^c$  and constraint was then calculated using only those SENB results corresponding to cleavage fracture ( $\Delta a < 0.2\text{mm}$ ), to match the conditions under which the uniaxial wide plate test had failed. For this second set of data, a simple straight line with  $\alpha=0.533$ ,  $m=1$ ,  $K_{mat}=180\text{MPa}\sqrt{\text{m}}$  was used.

The constraint-modified FAD for analysis of the uniaxial wide plate is shown in Fig.13. The failure analysis line derived from all data ( $\alpha=14.4$ ,  $m=5.52$ ) rises very rapidly above  $L_r \approx 0.5$ ; the CTOD-based constraint analysis safely predicts failure, whilst the  $K_J$ -based analysis does not. Given the very steep rise in the failure analysis line, small changes in the assumed value of  $L_r$  could shift the analysis points either side of the line. The failure analysis line derived from cleavage data only ( $\alpha=0.533$ ,  $m=1$ ) also passes between the CTOD-based and  $K_J$ -based points, giving a safe analysis only if the CTOD toughness parameter is used.

A similar analysis can be carried out for the biaxial wide plate test, as shown in Fig.14. Results are shown for  $\alpha=0.533$ ,  $m=1$  only, since the  $\alpha=14.4$ ,  $m=5.52$  line virtually coincides with the standard failure assessment line (the  $-\beta_T L_r^m$  term is close to zero). It can be seen that the  $K$ -based assessment point virtually coincides with the failure analysis line. The effects of biaxiality on the failure assessment line are fairly small at small  $L_r$  values, as would be expected from the accuracy of the standard FAD-based analysis shown in Fig.11. Nevertheless, the constraint-based method shows that at higher values of  $L_r$ , a substantial enlargement of the 'safe' area of the FAD would be expected under biaxial loading.

### 4.5. OVERALL DISCUSSION

From the above analysis, it can be seen that a constraint-based analysis can provide a more accurate prediction of the failure condition of wide plate tests, compared with a standard FAD-based approach. Nevertheless, the programme has highlighted a number of potential difficulties:

1. Firstly, a large number of datapoints is needed to provide a consistent relationship between fracture toughness and the constraint parameter  $T/\sigma_Y$ , since data scatter is high under conditions of high fracture toughness/low constraint.
2. The indications from this work are that Procedure II (modification of  $K_r$ ) is easier to follow than Procedure I (modification of the FAD), since a lower-bound toughness for a particular value of  $T/\sigma_Y$  is more easily determined by eye than by curve-fitting.
3. Whichever procedure is used, a choice must be made between the various solutions available in the literature for stress intensity, T-stress, plastic collapse and shallow-crack fracture toughness, and the outcome of a constraint-based analysis could be critically dependent on which solution is used.

## EFFECT OF CRACK TIP CONSTRAINT ON FRACTURE TOUGHNESS OF A533B STEEL AND VALIDATION OF THE SINTAP CONSTRAINT PROCEDURE

4. The wide plate tests described consisted of plain material only; in considering more structurally relevant welded components, the effects of thermal and residual stresses, misalignment, strength mismatch and microstructure would need to be taken into account. It is understood that Appendix 14 has not been validated against such cases at the time of writing.

As shown in Section 4.4.1-4.4.3, test results were always correctly predicted when a standard FAD and lower-bound values of toughness were used; when constraint-based procedures were used, only the analysis based on lower-bound CTOD safely predicted failure, whilst the analysis from lower-bound values of  $K_J$  incorrectly predicted survival in some cases. This may be due in part to underestimation of the true driving force; thermal stresses probably also played a role in the fracture of the uniaxial wide plate, but have not hitherto been analysed. Thermal analysis of the uniaxial plate, and additional analysis of the surface-cracked biaxial wide plate tests carried out on the same material, would provide further validation of the method.

### 5. CONCLUDING REMARKS

1. Twenty fracture toughness tests have been carried out on a grade A533B steel identical to that used in a series of low-temperature wide plate tests. All tests were carried out using single edge-notched bend (SENB) specimens at a temperature of  $-100^{\circ}\text{C}$ . Crack depth was varied between 5 and 25mm, giving  $a_0/W$  ratios between 0.1 and 0.5; the critical value of  $J$  at fracture was calculated from the draft ASTM procedure for shallow crack tests.
2. Low-constraint (shallow-crack) specimens showed values of toughness up to four times higher than that associated with standard deeply-notched specimens. The highest values of toughness (and lowest values of  $a_0/W$ ) were associated with ductile tearing of up to 0.8mm on the specimen surface, whereas standard deeply-notched specimens failed by cleavage without prior ductile tearing.
3. Results of the programme were used in the interpretation of a series of wide plate tests carried out by TWI. The methods described in Appendix 14 of R6 and Appendix 3 of the draft SINTAP procedure were used to index the measured fracture toughness in terms of constraint parameters  $T/\sigma_Y$  and  $Q/\sigma_Y$ . Results for the wide plate specimens and SENB specimens were shown to lie on the same fracture toughness/constraint locus, providing an experimental validation of Procedure II of Appendix 14.
4. Uniaxial and equibiaxial wide plate tests were also analysed using a constraint-based FAD, in accordance with Procedure I of Appendix 14. The exact form of the relationship between  $K_{mat}$  and  $T/\sigma_Y$  was difficult to determine unambiguously, because of the very steep rise in fracture toughness associated with very negative  $T$ -stress and increasing amounts of stable ductile tearing in the SENB specimens. Nevertheless, the constraint-based FAD safely predicted the failure of the wide plate tests, provided that lower-bound values of CTOD were used. Lower-bound values of  $J$  produced analysis points just inside the failure analysis line, i.e. the predictions were slightly non-conservative.

**6. REFERENCES**

- 1** Milne I, Ainsworth R A, Dowling A R and Stewart A R: 'Assessment of the integrity of structures containing defects'. CEGB Report R/H.R6-Rev.3, LEGB, 1986
- 2** PD6493 BSI PD6493:1991: 'Guidance on methods for assessing the acceptability of flaws in fusion welded structures'. British Standards Institution, London, 1991.
- 3** BS 7910:1999 'Guidance on methods for assessing the acceptability of flaws in structures'. British Standards Institution, London, 1999 (to be published).
- 4** SINTAP Appendix 3.
- 5** Hadley I: 'Constraint differences between specimens and real structures', TWI Report 220630/1/96. March 1996.
- 6** Andrews R M and Garwood S J: 'Testing of A533B under equibiaxial loading with a through-thickness crack'. TWI Report No. 34121/1/94, August 1994.
- 7** Garwood S J and Andrews R M: 'Testing of a further A533B wide plate under biaxial loading with a through-thickness crack - Preliminary analysis'. TWI Report 220548/1/95, May 1995.
- 8** Andrews R M: 'Testing of a further A533B wide plate under biaxial loading with a through-thickness crack – Temperature profiles'. TWI Report 220548/2/95, November 1995.
- 9** Challenger N V and Andrews R M: 'Biaxial test programme – Through-thickness cracked uniaxial wide plate test on A533B material'. TWI Report 220682/1/96, March 1996.
- 10** Andrews R M, Noblett J E and Garwood S J: 'Further analysis of a through-thickness notched biaxial fracture test', TWI Report No. 34106/1/94, January 1995.
- 11** Challenger N V and Dickerson T L: 'Further analysis of through-thickness notched biaxial fracture tests'. TWI Report No. 220683/1/96, April 1996.
- 12** Dawes M G, Slater G, Gordon J R and McGaughy T H: 'Shallow crack test methods for the determination of  $K_{Ic}$  CTOD and J fracture toughness'. Shallow Crack Fracture Mechanics, Toughness Tests and Applications Conference, TWI, Cambridge 23-24 September 1992.
- 13** Draft annex to ASTM E1290 Revision 6, August 1998.
- 14** WRC Bulletin 418 January 1997: 'Constraint effects on fracture behaviour', (three reports by J A Smith and S T Rolfe).

**EFFECT OF CRACK TIP CONSTRAINT ON FRACTURE TOUGHNESS OF A533B STEEL AND VALIDATION OF THE SINTAP CONSTRAINT PROCEDURE**

- 15** Neale B K: 'Evaluation of constraint in fracture toughness test specimens', Nuclear Electric Report No. EPD/GEN/REP/0295/98, Issue 1.
- 16** Sanderson D J, Sherry A H and O'Dowd N P: 'Compendium of  $\beta$  solutions for use with the R6 constraint modified framework', AEA report AEA-TSD-0981, May 1996.
- 17** Sherry A H, France C C and Goldthorpe M R: 'Compendium of T-stress solutions for two- and three-dimensional cracked geometries'. *Fatigue and Fracture of Engineering Materials & Structures*, **18** (1), 141-155, 1995.
- 18** Andrews R M and Garwood S J: 'An analysis of fracture under biaxial loading using the non-singular T-stress', ASTM Symposium, Fort Worth, Dallas, USA, 17-18 November 1993.
- 19** Goldthorpe M R and Wiesner C S: 'Further development of an improved definition of upper shelf behaviour: revised final report'. TWI Report 220735/5a/97.
- 20** Schwalbe K-H and Neale B: 'A procedure for determining the fracture behaviour of materials – the unified fracture mechanics test method EFAM GTP 94', *Fatigue and Fracture of Engineering Materials and Structures* 18/4, 1995, 413-424, also published as Report No. GKSS 94/E/60
- 21** Challenger N V, Phaal R and Garwood S J: 'Appraisal of PD6493:1991 fracture assessment procedures - Part I – TWI data'. TWI Members' Report 512/1995.

**EFFECT OF CRACK TIP CONSTRAINT ON FRACTURE TOUGHNESS OF A533B STEEL AND  
VALIDATION OF THE SINTAP CONSTRAINT PROCEDURE**

**TWI ENDORSEMENT**

This work has been carried out in accordance with TWI's QA Procedures.

Project Leader ..... Head of Department .....  
(or delegate)

## EFFECT OF CRACK TIP CONSTRAINT ON FRACTURE TOUGHNESS

**Table 1** Results of fracture mechanics tests on SENB specimens

Specimen ID	$a_0/W$	Type of result*	Ductile tear length, $\Delta a$ ,mm	$J_{BS}$ , kJ/m <sup>2</sup>	$J_q$ ,kJ/m <sup>2</sup>	CTOD <sub>BS</sub> , mm
220682 M01-01**	0.480	c	0.00	116.0***	-	0.110
220682 M01-02**	0.481	c	0.00	82.0	-	0.079
220682 M01-03**	0.478	c	0.10	276.6	-	0.271
8269 M01-01	0.476	c	0.05	107.9	108.8	0.125
8269 M01-02	0.158	c	0.11		196.0	
8269 M01-03	0.098	u	0.30		343.3	
8269 M01-04	0.232	c	0.00		66.3	
8269 M01-05	0.130	c	0.00		285.9	
8269 M01-06	0.103	c	0.14		222.5	
8269 M01-07	0.469	c	0.19	207.8	220.5	0.225
8269 M01-08	0.172	c	0.17		216.2	
8269 M01-09	0.087	u	0.78		801.4	
8269 M01-10	0.238	c	0.17		242.3	
8269 M01-11	0.119	u	0.56		685.4	
8269 M01-12	0.100	u	0.27		294.3	
8269 M01-13	0.491	c	0.10	108.2	111.9	0.111
8269 M01-14	0.154	u	0.38		327.7	
8269 M01-15	0.092	u	0.56		553.9	
8269 M01-16	0.240	c	0.00		214.8	
8269 M01-17	0.130	c	0.13		248.5	
8269 M01-18	0.108	u	0.25		340.9	
8269 M01-19	0.335	c	0.09		206.8	
8269 M01-20	0.325	u	0.23		285.6	

**Note:**

\* Under 'Type of result', 'c' designates that the specimen failed in an unstable manner, with less than 0.2mm of ductile tearing on the fracture surface. 'u'; designates unstable fracture with more than 0.2mm of ductile tearing on the fracture surface.

\*\* Results refer to rectangular-section (50x100mm) SENB specimens tested in a previous project

\*\*\* J from single clip result only

## EFFECT OF CRACK TIP CONSTRAINT ON FRACTURE TOUGHNESS

**Table 2** Results of tests on CCT wide plate specimens tested at  $-100^{\circ}\text{C}$ ; mean value for deeply-notched SENB specimens also shown for comparison

Test ID	Biaxiality ratio, k	2a, mm	B, mm	2W, mm	a/W	$\sigma_g$ at failure, N/mm <sup>2</sup>	CTOD, mm*
220682/M01-28	0 (uniaxial)	200	51	500	0.400	271	0.35
220548/M01-27b	0.5	203	51	500	0.406	189	0.1
220682/M01-26	1 (equibiaxial)	203	51	500	0.406	149	0.1
220548/M01-27a	1.9	203	51	500	0.406	133**	0.05**
deeply-notched SENB	-	-	50	-	-	-	0.15 (average of six)

**Note:**  $\sigma_g$  is the applied stress perpendicular to the notch at failure

\* CTOD measured directly from clip gauges placed across the crack tip

\*\* did not fail under these conditions; subsequently reloaded to  $k=0.5$  (see M01-27b)

**Table 3** Constraint and collapse parameters for the wide plate specimens

ID	k	a/W	$\sigma_Y$ , N/mm <sup>2</sup>	$\sigma_L$ , N/mm <sup>2</sup>	$L_r = \sigma_g / \sigma_L$	$\beta_T$	$\beta_T L_r$ (Ref. 16)	$T/\sigma_Y$ (Ref. 17)	$T/\sigma_Y$ (Ref. 19)
M01-28	0 (uniaxial)	0.400	604	418.5	0.648	-0.802	-0.519	-0.510	-0.488
M01-27	0.5	0.406	604	-	-	-	-	-	-0.140
M01-26	1 (equibiaxial)	0.406	604	697.4	0.214	-0.318	-0.068	-0.053	0.047
M01-27	1.9	0.406	604	-	-	-	-	-	0.323

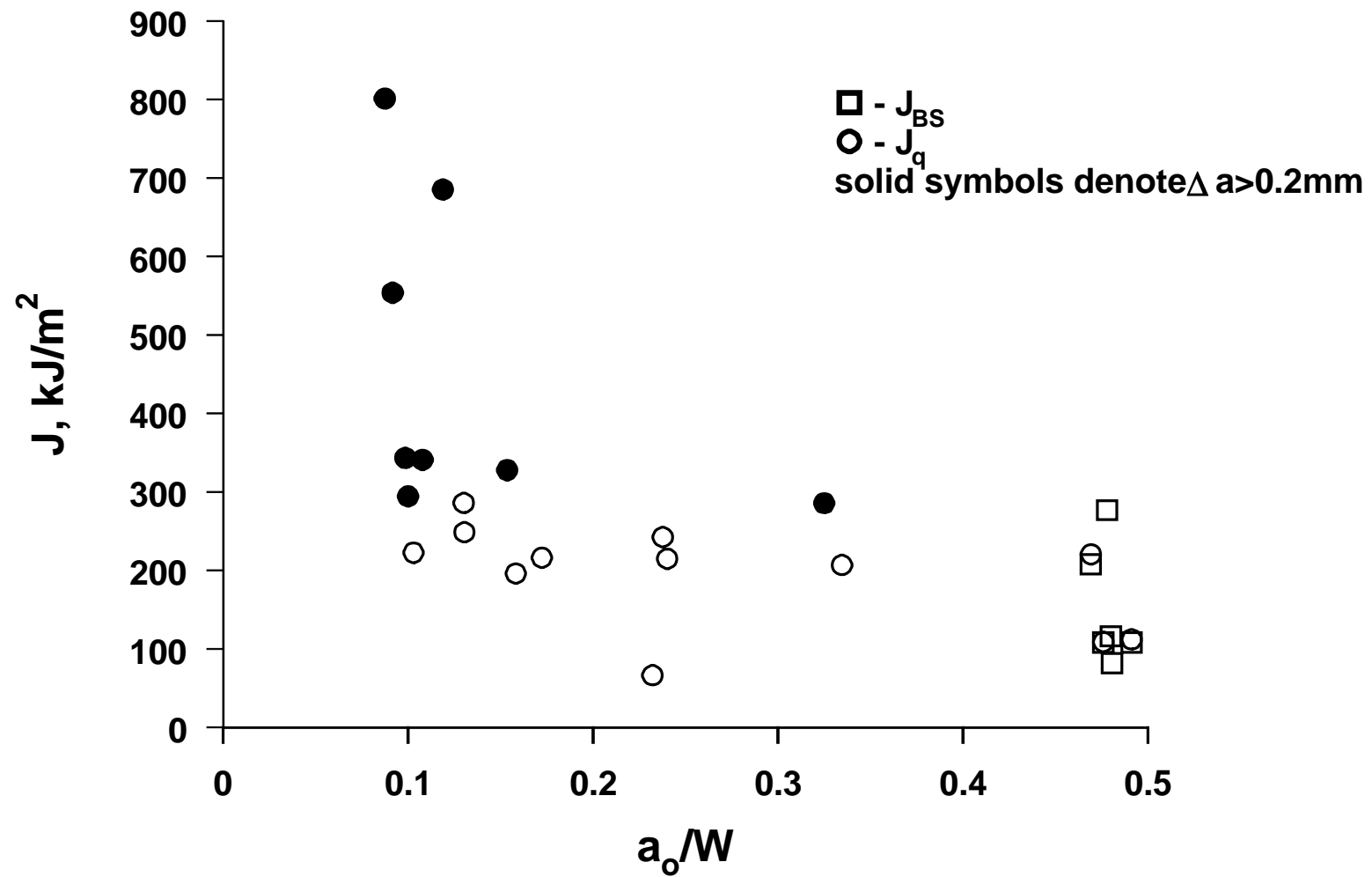


Fig.1 Relationship between fracture toughness and crack depth (SENB specimens)

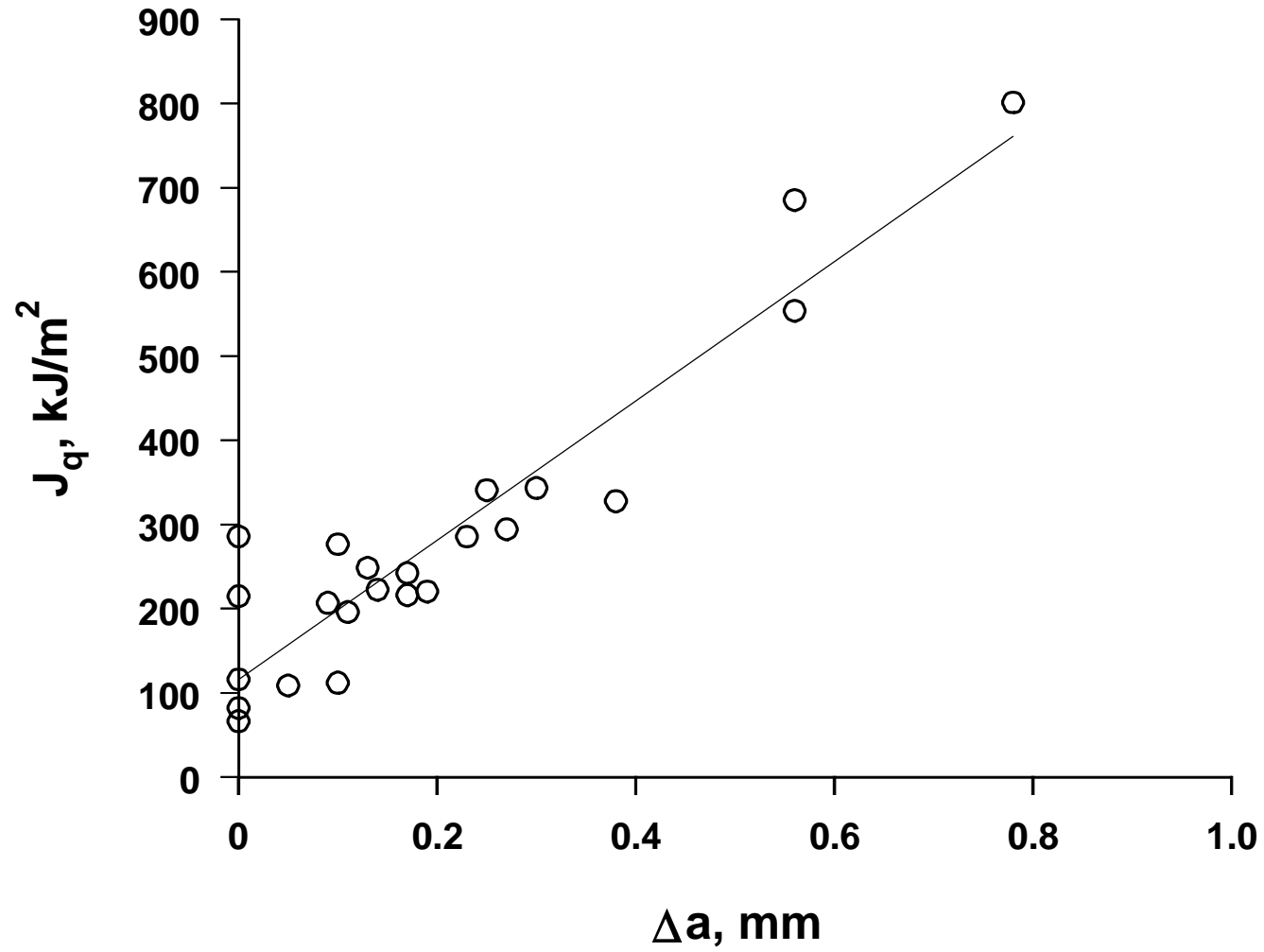
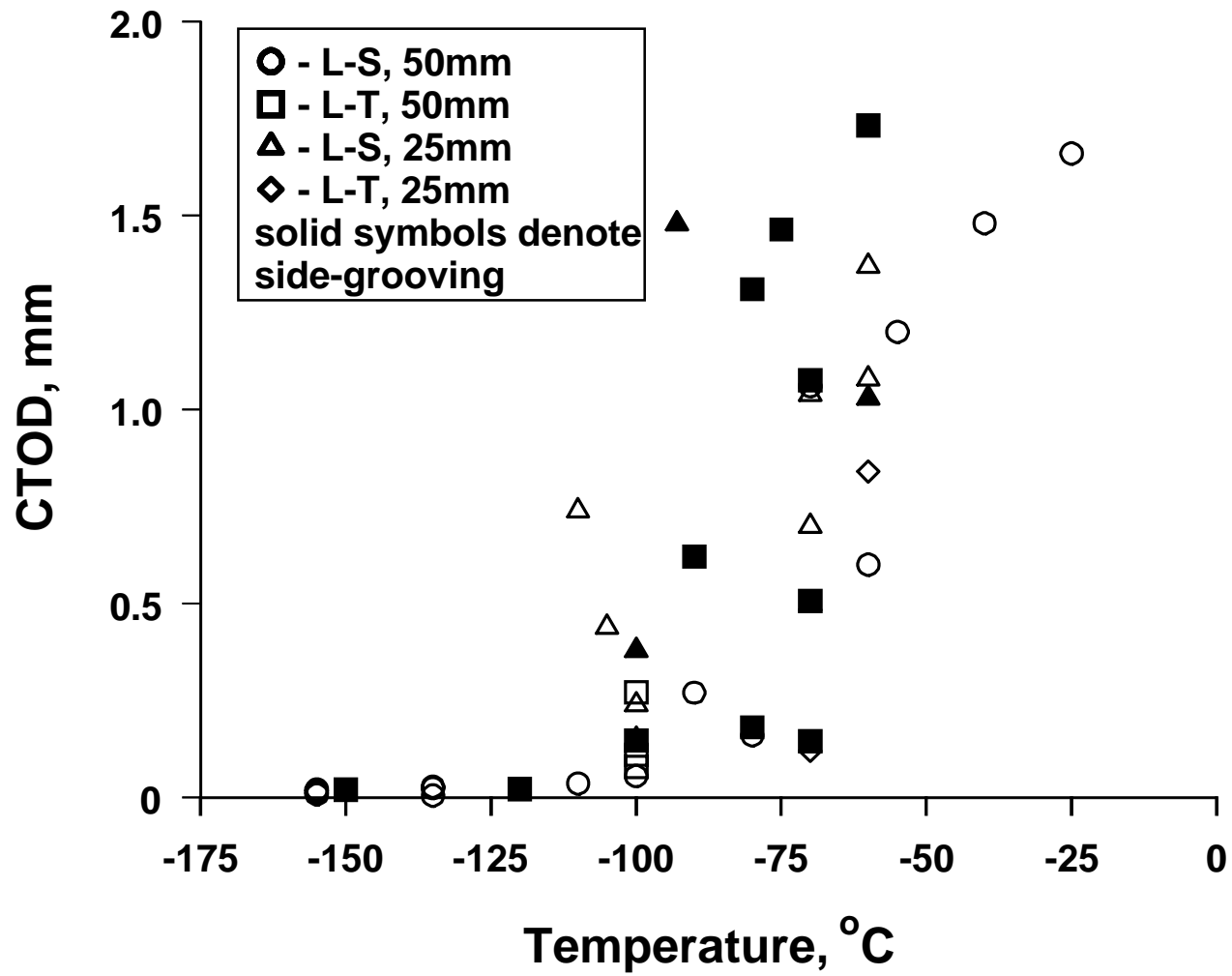


Fig.2 Relationship between fracture toughness and tear length (SENB specimens)



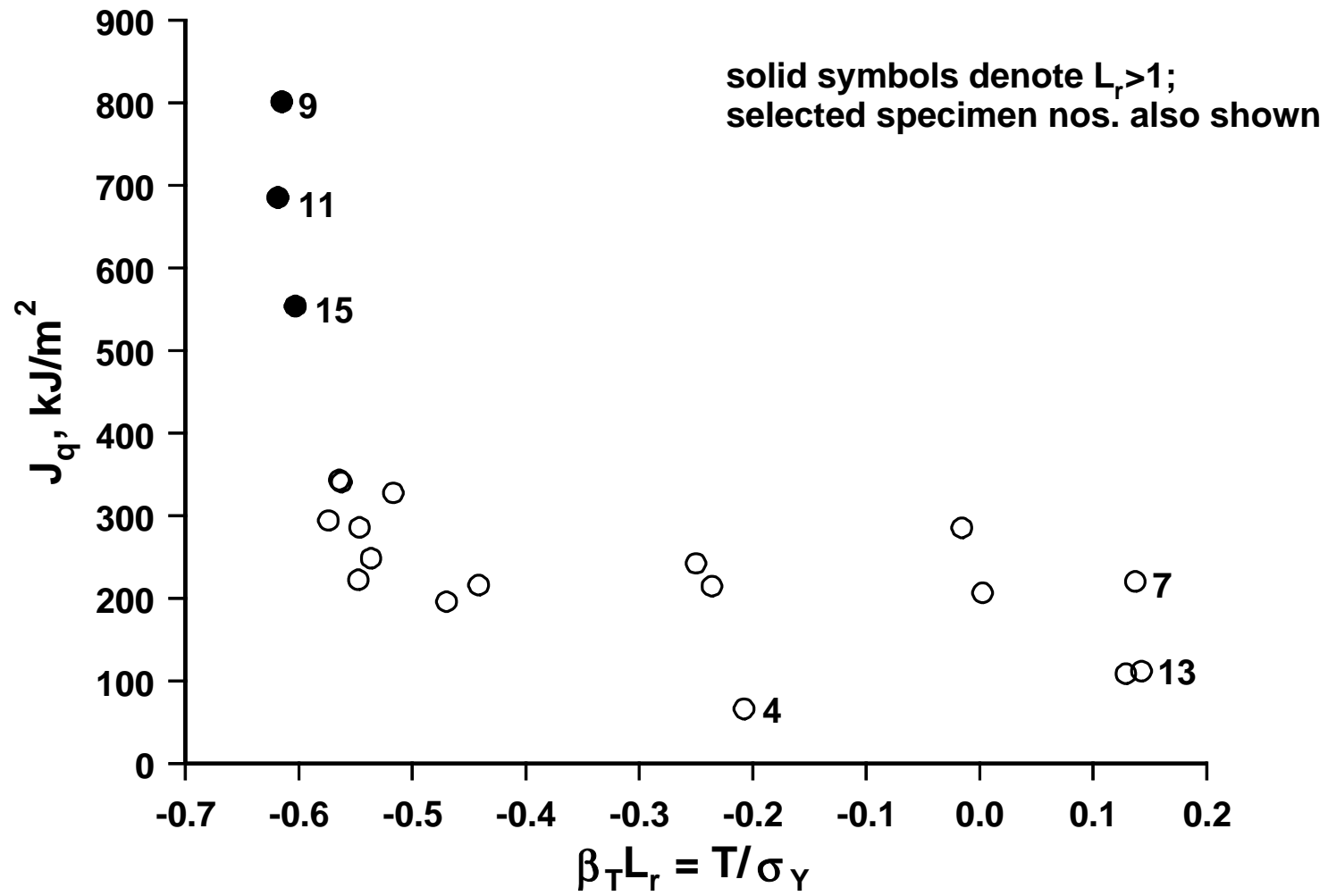


Fig.4 Relationship between fracture toughness and  $\beta_T L_r$  (SENB specimens)

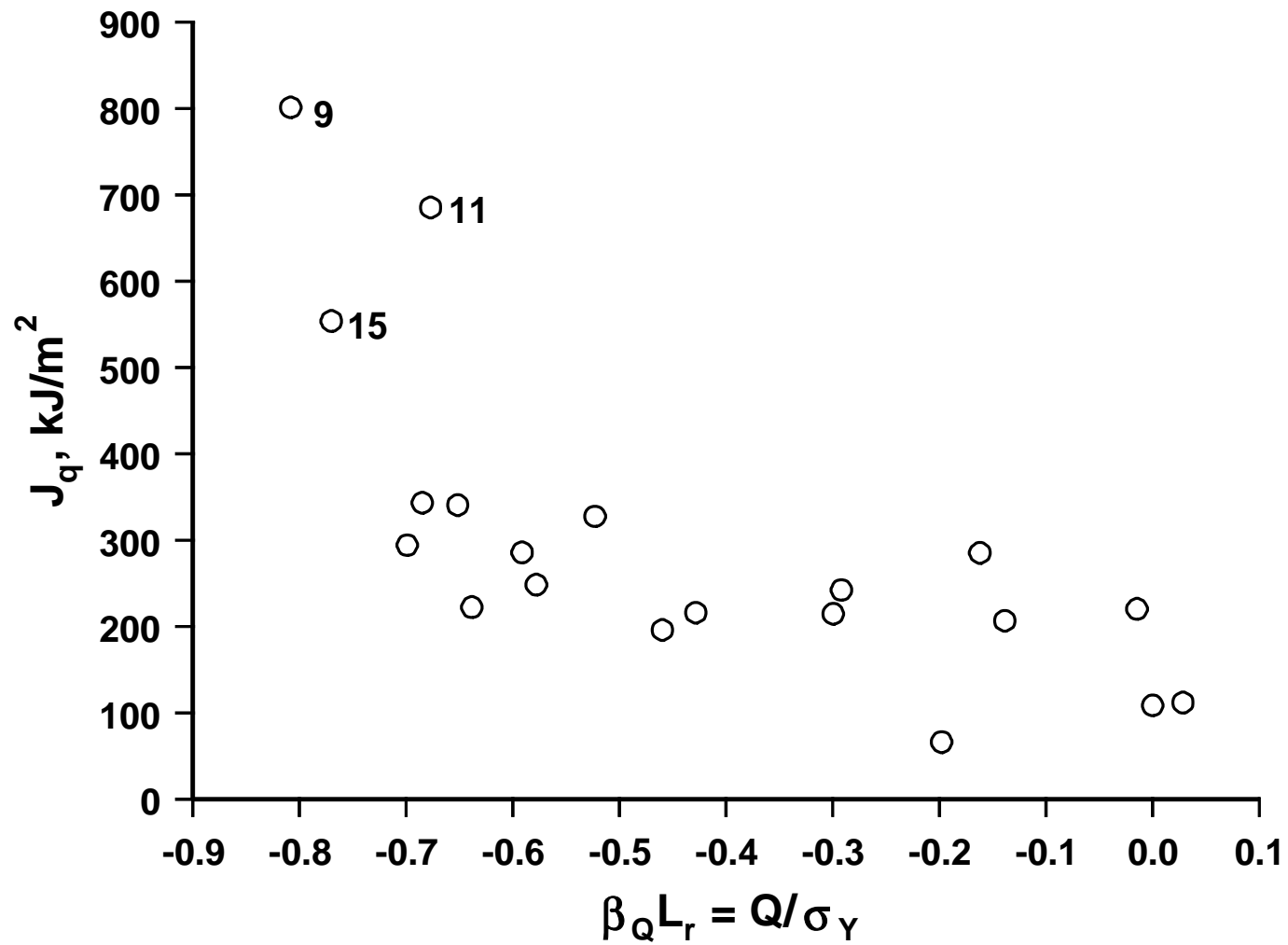
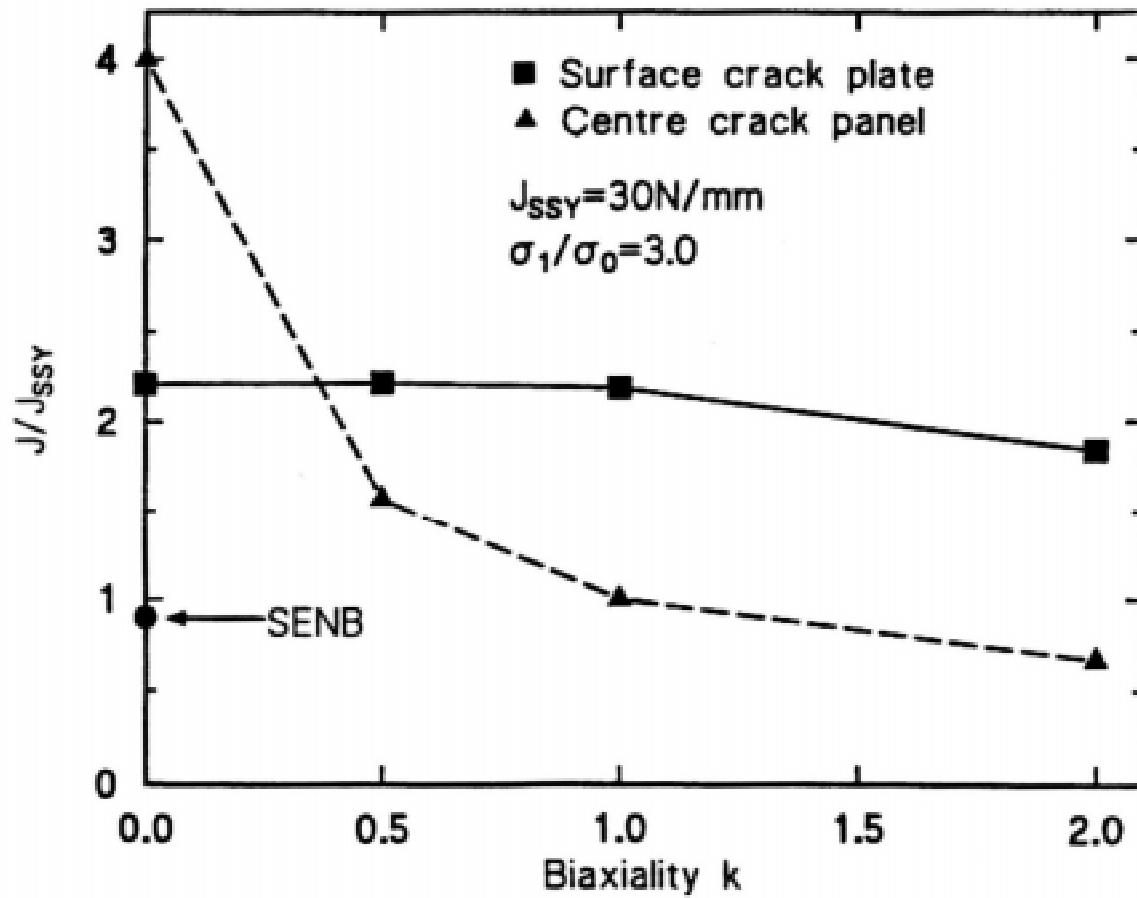


Fig.5 Relationship between fracture toughness and  $\beta_Q L_r$  (SENB specimens)



**Fig.6 Predicted effect of biaxial loading on cleavage toughness (ref. 18)**

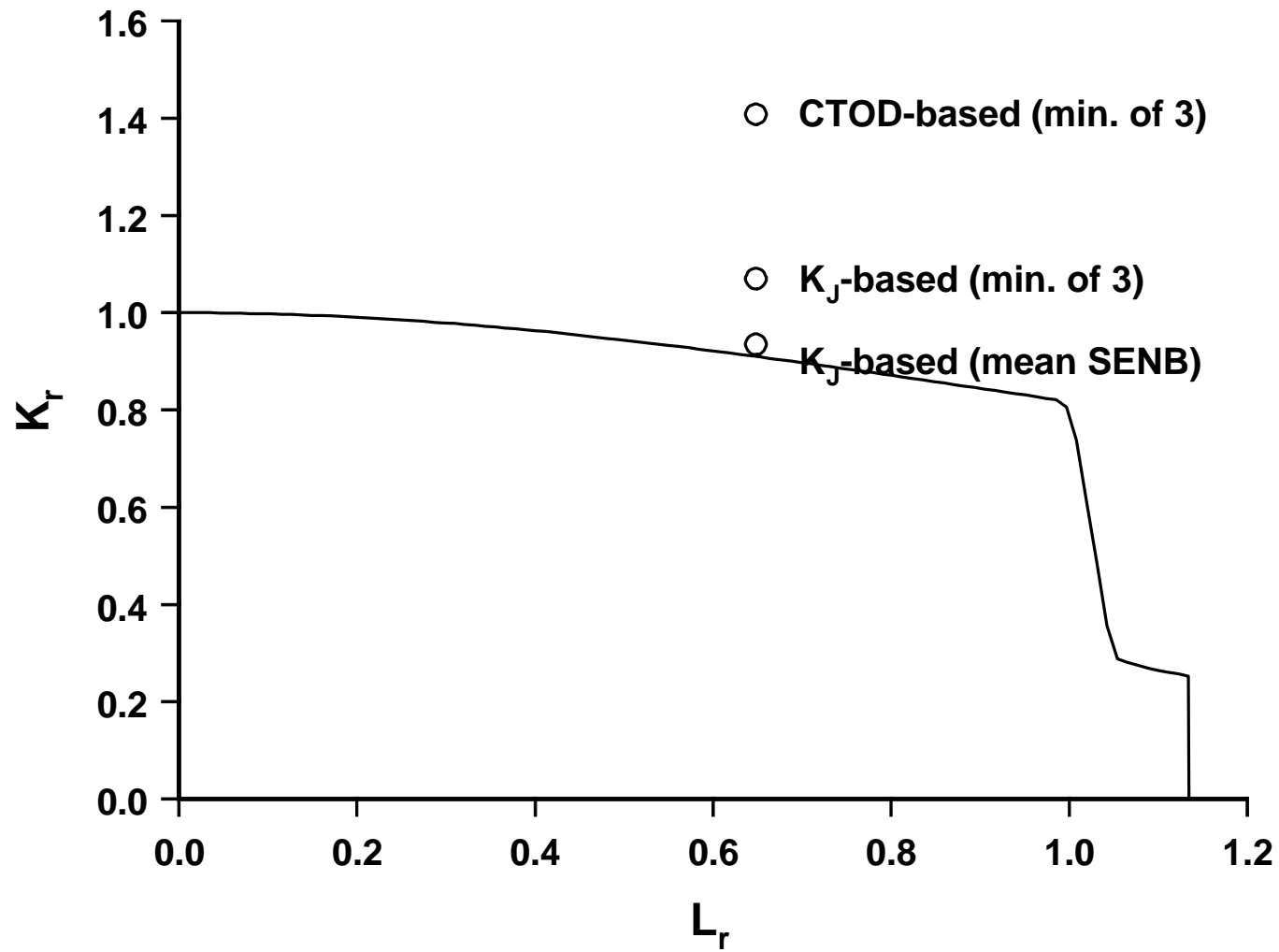


Fig.7 Standard FAD-based analysis of uniaxial wide plate test

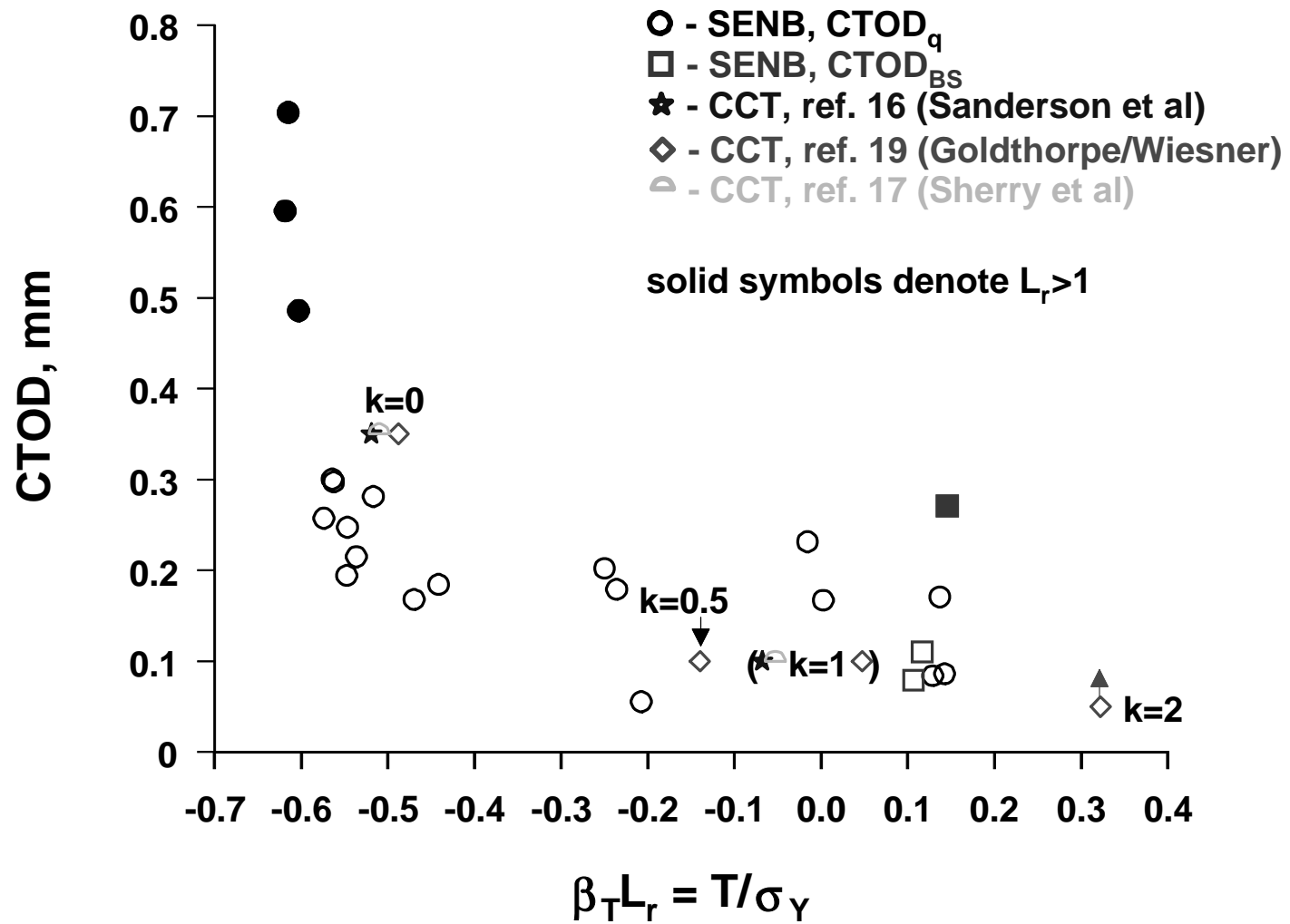


Fig.8 Results of wide plate (CCT) and SENB tests in terms of CTOD

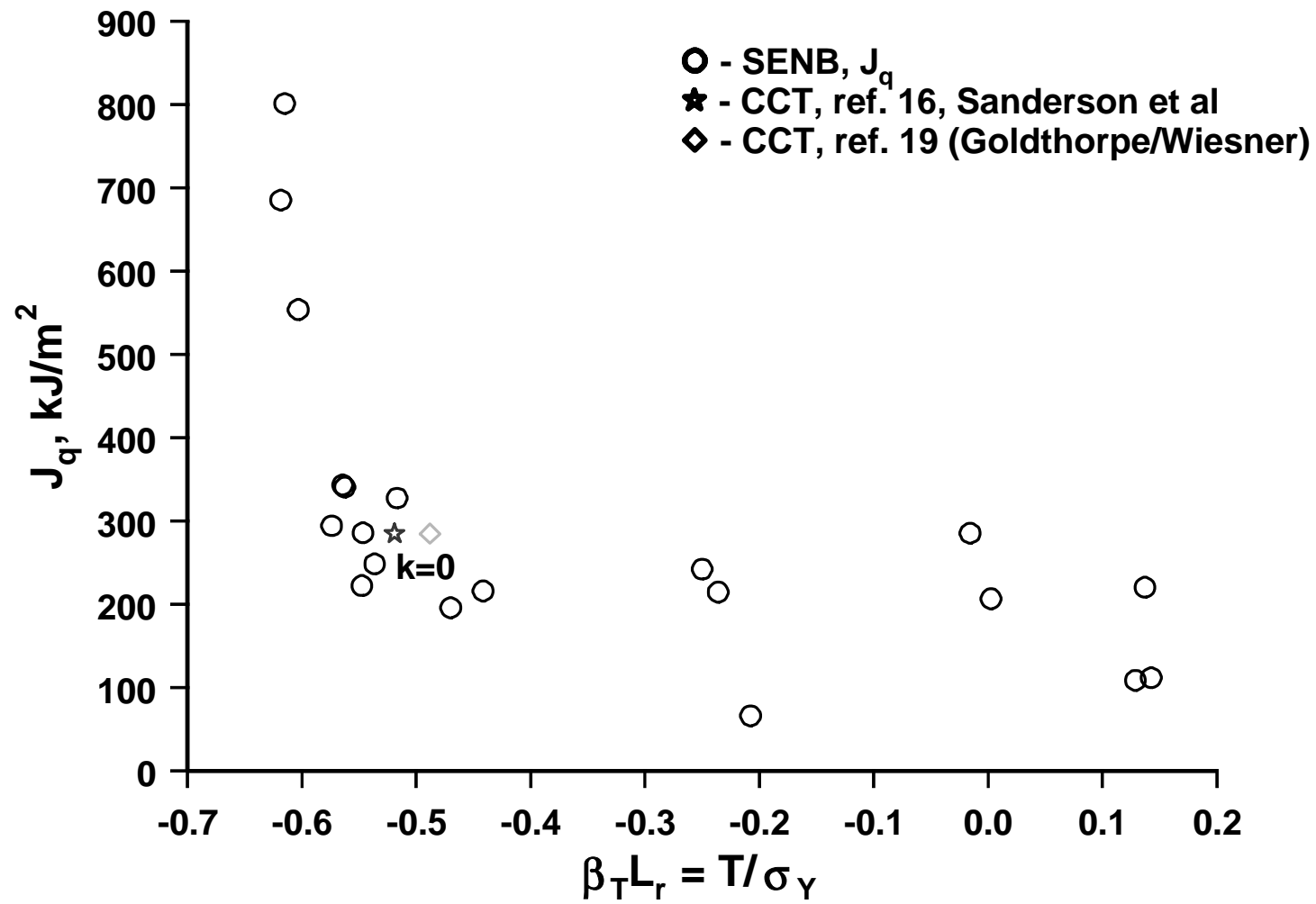


Fig.9 Results of uniaxial wide plate (CCT) test and SENB tests in terms of J

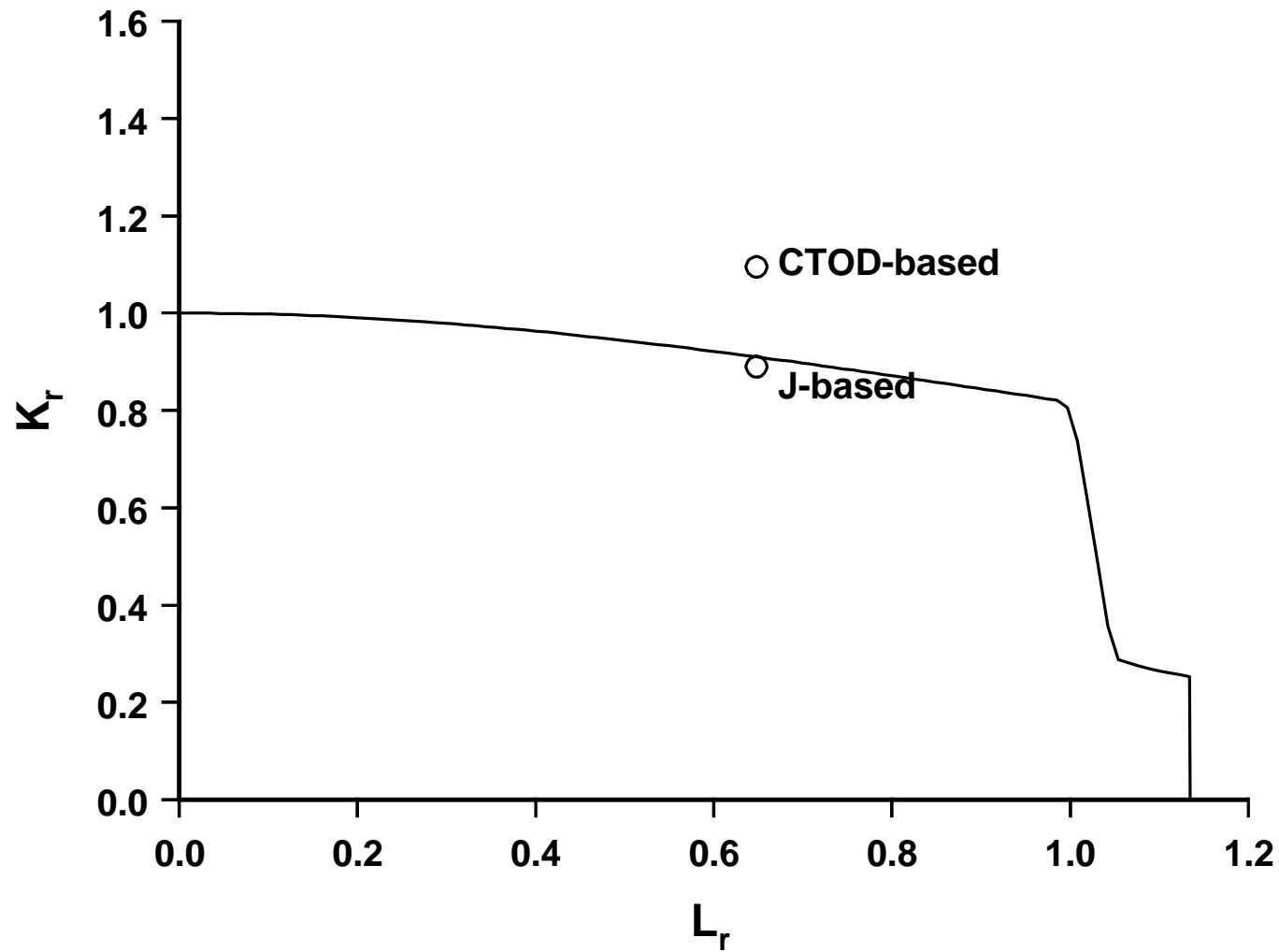


Fig.10 Analysis of uniaxial WP test using standard FAD and low-constraint SENB data

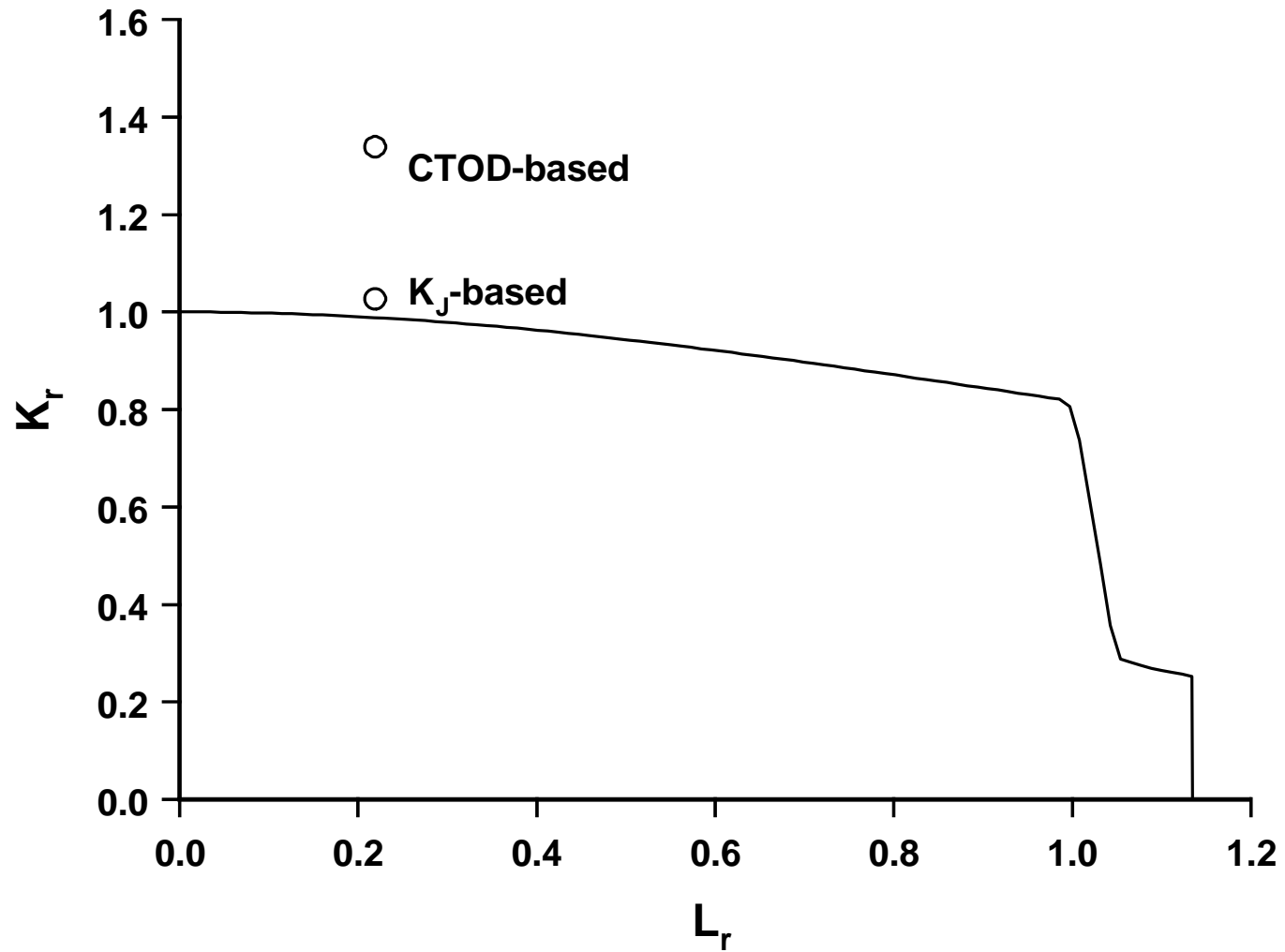


Fig.11 Standard FAD-based analysis of equibiaxial wide plate test

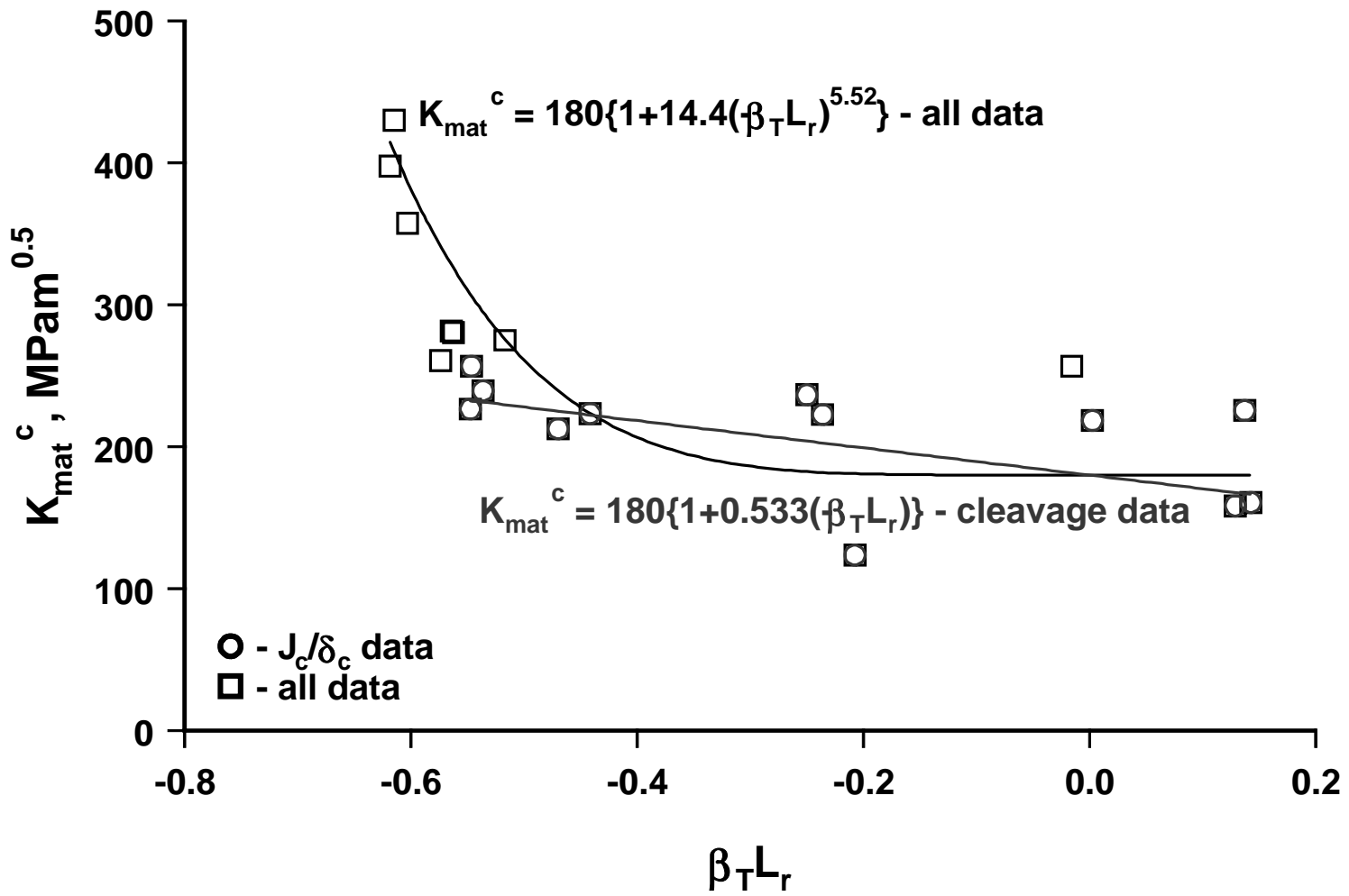


Fig.12 Best fit to  $K_{mat}$  (SENB data)

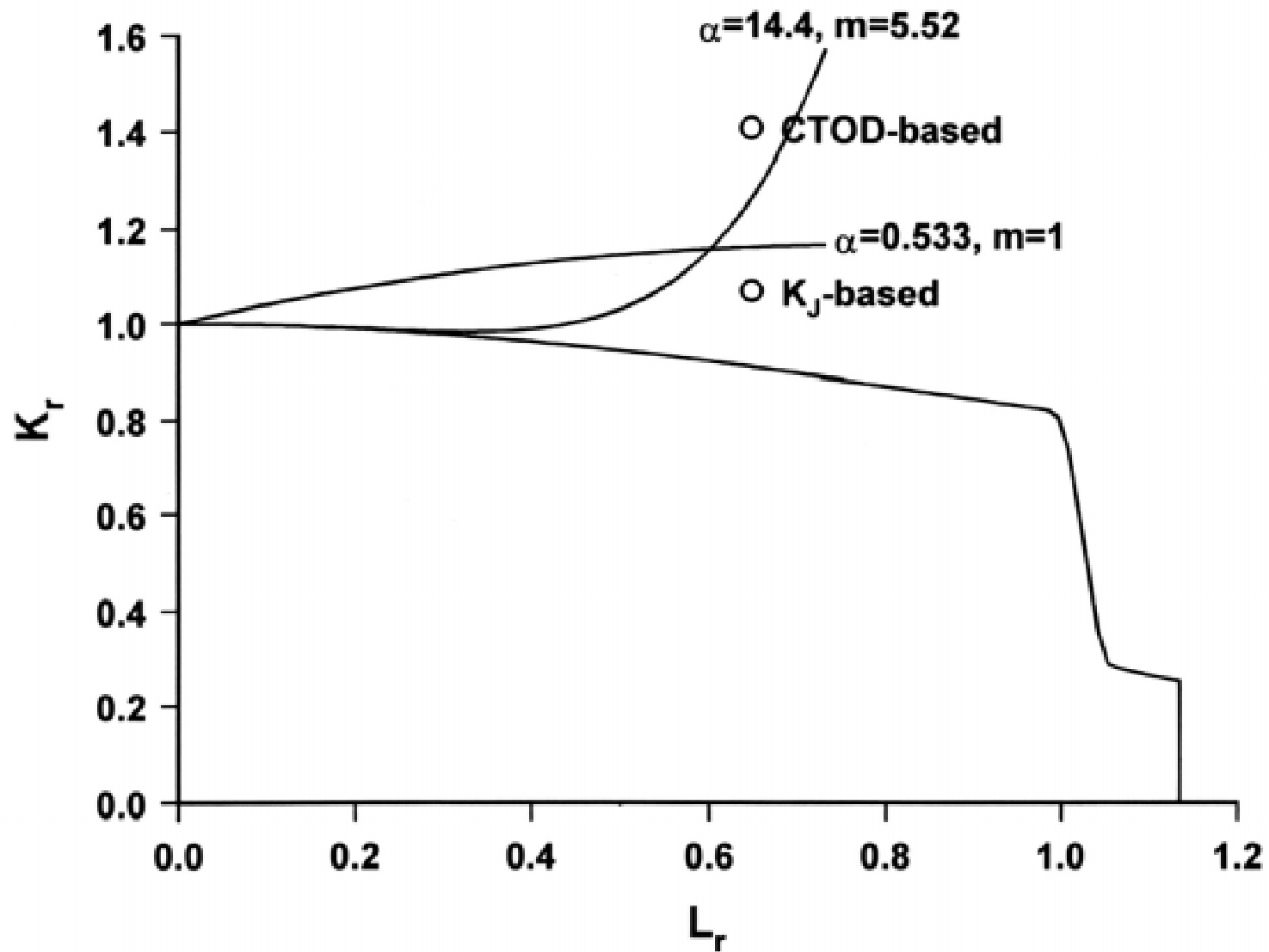


Fig.13 Use of a modified FAD to analyse uniaxial wide plate test results

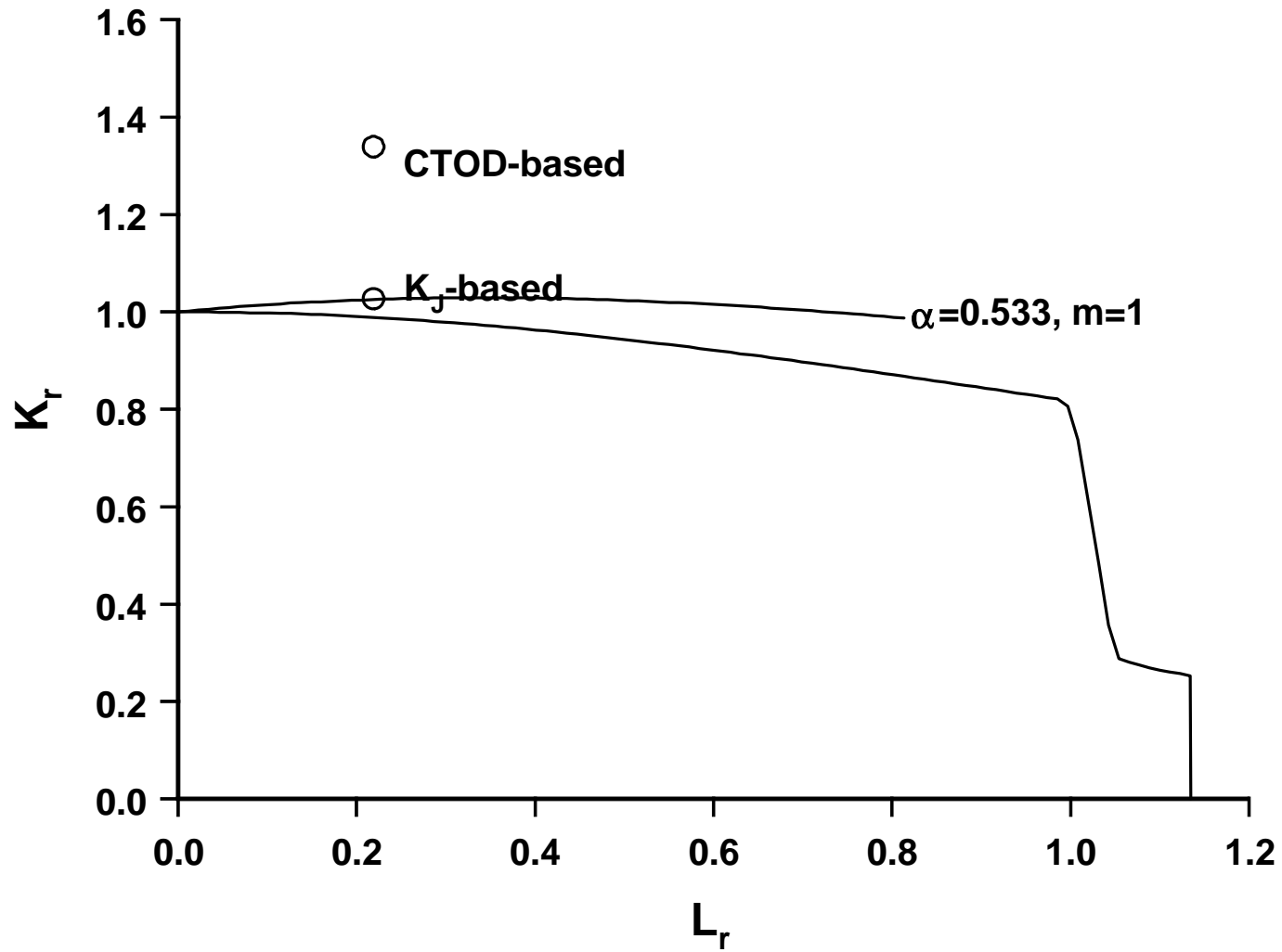


Fig.14 Use of a modified FAD to analyse biaxial wide plate test results